Multimode anharmonic third-order harmonic generation in a photonic-crystal fiber

A. A. Ivanov,[1,2] D. Lorenc,[3] I. Bugar,[3] F. Uherek,[3] E. E. Serebryannikov,[4] S. O. Konorov,[4] M. V. Alfimov,[2] D. Chorvat,[3] and A. M. Zheltikov[1,4]

[1]*International Laser Center, M. V. Lomonosov Moscow State University, Vorob'evy gory, 119992 Moscow, Russia*

[2]*Center of Photochemistry, Russian Academy of Sciences, Novatorov 7a, 117421 Moscow, Russia*

[3]*International Laser Center, Ilkovičova 3, 81219 Bratislava, Slovak Republic*

[4]*Physics Department, M. V. Lomonosov Moscow State University, Vorob'evy gory, 119992 Moscow, Russia*

(Received 28 January 2005; revised manuscript received 28 September 2005; published 18 January 2006)

While the third harmonic of a monochromatic pump field with a frequency ω_0 is generated exactly at the frequency $3\omega_0$, frequency tripling of broadband ultrashort pump pulses in extended nonlinear media tends to generate isolated spectral peaks substantially shifted from $3\omega_0$. We demonstrate this phenomenon by studying nonlinear spectral transformations of femtosecond Cr:forsterite laser pulses in multimode photonic-crystal fibers. Third-harmonic generation is shown to map adjacent guided modes of the third harmonic onto a manifold of spectral peaks within a 150-THz range around $3\omega_0$. The spectral shifts and the widths of these peaks are controlled by the phase and group-velocity mismatch between the pump field and third-harmonic modes, as well as the length of nonlinear-optical interaction and broadening of the pump spectrum, allowing the spectral content of the third-harmonic signal to be engineered by tailoring the fiber dispersion.

DOI: 10.1103/PhysRevE.73.016610 PACS number(s): 42.70.Qs, 42.65.Wi, 42.81.Qb

Third-harmonic generation (THG) is one of the basic nonlinear wave phenomena observed in various areas of nonlinear physics, including fluid mechanics, plasma physics, and electrodynamics [1–3]. In optics, THG has been known and employed for frequency conversion and spectroscopic applications from the early days of the laser era [4]. For monochromatic waves, energy conservation dictates the relation $3\omega_0=\omega_0+\omega_0+\omega_0$ between the frequency ω_0 of the incoming wave, referred to as the pump, and the frequency $3\omega_0$ of the third harmonic. A broad bandwidth of short field waveforms adds an uncertainty to the THG energy conservation relation, with the mapping between the pump and third-harmonic spectra controlled by the regime of nonlinear-optical interaction. Momentum conservation, known as phase matching in nonlinear optics, and nonlinear phase shifts of the pump and third-harmonic fields have been identified [5,6] as the main physical factors influencing the spectrum of the third harmonic in ultrafast nonlinear optics. Both momentum mismatch and nonlinear phase shifts accumulate with propagation distances. The mapping between the pump and third-harmonic spectra can therefore become especially complicated in waveguide regimes of nonlinear-optical interactions. Recently invented photonic-crystal fibers (PCFs) [7–9] provide a radical enhancement of nonlinearities due to the field confinement in the fiber core [9] and allow dispersion profiles of guided modes to be tailored by PCF structure engineering [10], leading to large coherence lengths of nonlinear-optical interactions. THG has been shown to display interesting new features under these conditions. Asymmetric spectral broadening of the third-harmonic spectrum and noticeable spectral shifts of the third harmonic have been observed in recent experiments with fused silica [11–16] and soft-glass [17] PCFs, as well as with tapered fibers [18].

In this work, we demonstrate that, unlike THG in a monochromatic pump field, frequency tripling of ultrashort pulses in extended nonlinear media tends to form isolated spectral peaks substantially shifted from the $3\omega_0$ frequency. We will investigate spectral transformations of femtosecond pulses of 1.24- to 1.25-μm Cr:forsterite laser radiation in multimode PCFs and show that THG maps adjacent guided modes of the third harmonic onto a manifold of spectral peaks within a 140-THz range around $3\omega_0$. The spectral shifts and the widths of these peaks are controlled in this regime by the phase and group-velocity mismatch between the pump field and third-harmonic modes, as well as the length of nonlinear-optical interaction and broadening of the pump spectrum, allowing the spectral content of the third-harmonic signal to be engineered by tailoring the fiber dispersion.

We start with qualitative arguments illustrating phase matching for THG generalized to include the phase and group-velocity mismatch of the pump and third-harmonic fields. We represent the propagation constants β_p and β_h of guided modes at the frequencies of the pump field and the third harmonic as

$$\beta_p(\omega) \approx \beta(\omega_0) + v_p^{-1}\Omega/3, \tag{1}$$

$$\beta_h(3\omega) \approx \beta(3\omega_0) + v_h^{-1}\Omega, \tag{2}$$

where ω_0 is the central frequency of the pump field, $v_{p,h-}=(\partial\beta/\partial\omega)^{-1}_{\omega_0,3\omega_0}$ are the group velocities of the pump and its third harmonic, and $\Omega=3\omega-3\omega_0$. In writing Eqs. (1) and (2), we neglect group-velocity dispersion and higher-order dispersion effects, as well as nonlinear phase shifts of the pump and third-harmonic fields induced through self- and cross-phase modulation. Using Eqs. (1) and (2), we write the phase mismatch for THG as

$$\Delta\beta = \beta_h - 3\beta_p \approx \Delta\beta_0 + \xi\Omega, \tag{3}$$

where $\Delta\beta_0=\beta(3\omega_0)-3\beta(\omega_0)$ is the phase mismatch of the pump and third-harmonic propagation constants at the central frequencies of these fields and $\xi=v_h^{-1}-v_p^{-1}$ is the group-velocity mismatch.

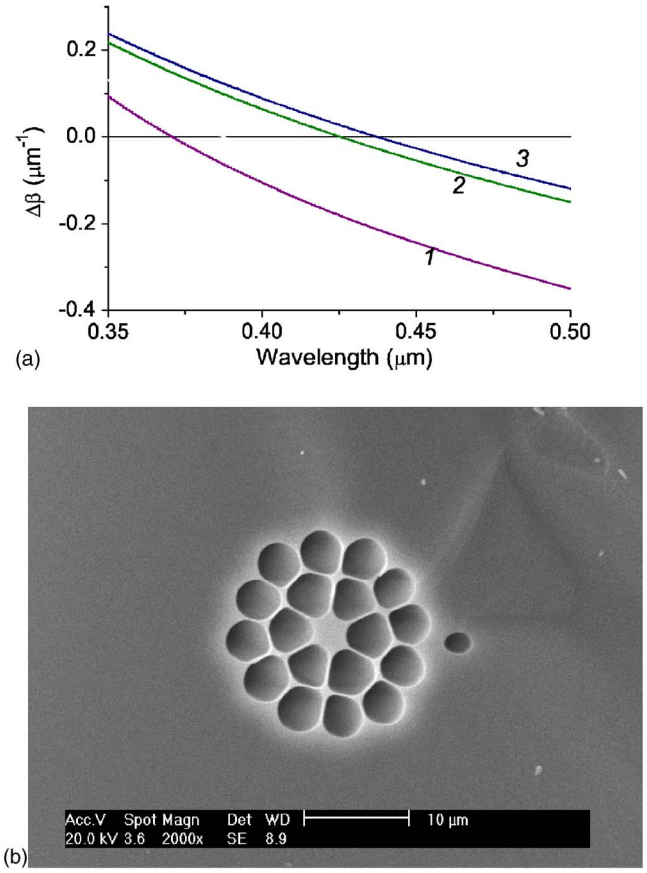

FIG. 1. (Color online) Mismatches of propagation constants $\Delta\beta$ calculated for the EH_{14} (curve 1), TE_{04} (2), and EH_{52} (3) modes of the third harmonic generated by the fundamental mode of 1.24 -μm pump radiation in an air-clad fused silica fiber with a core radius of 2 μm. The inset shows a scanning electron microscope image of the PCF employed in the experiments.

In a multimode regime of THG, the pump field coupled into a single (most often fundamental) guided mode can generate several guided modes of the third harmonic. Phase matching for a pair of third-harmonic modes is generally achieved at different frequency shifts Ω_1 and Ω_2 with respect to $3\omega_0$. The difference of Ω_1 and Ω_2 can be found from Eq. (3):

$$\Delta\Omega = \Omega_2 - \Omega_1 = \frac{\Delta\beta_{01}}{\xi_1} - \frac{\Delta\beta_{02}}{\xi_2}, \tag{4}$$

where $\Delta\beta_{0i}$ and ξ_i are the phase and group-velocity mismatch values for the first and second modes of the third harmonic $(i=1,2)$.

Figure 1 presents the phase mismatch calculated for the generation of the third harmonic of 1.24-μm Cr:forsterite laser radiation in a fiber consisting of a fused silica core with a radius of 2 μm and an air cladding. This simplified fiber model serves to illustrate the basic THG phase-matching options offered by a high-index-step fused silica PCF employed in our experiments (shown in the inset to Fig. 1), where the solid core is linked to the outer part of the cladding by thin submicrometer fused silica bridges. With the pump field

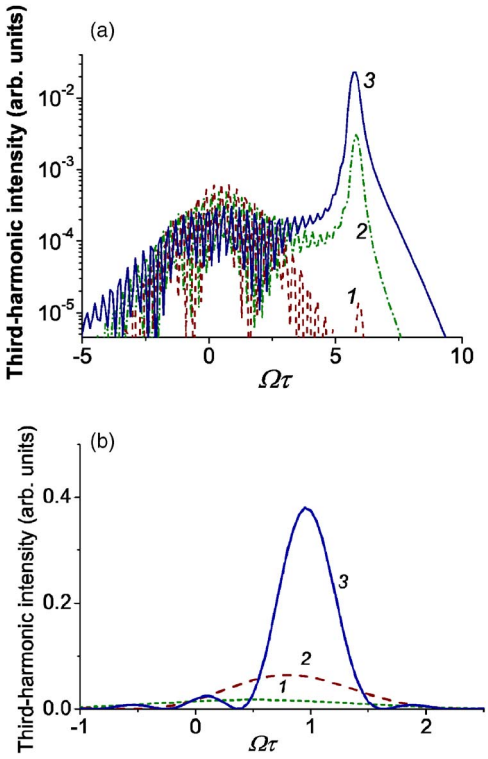

FIG. 2. (Color online) Spectra of the third harmonic generated with no SPM of the pump (curve 1) and with a SPM-broadened pump (curves 2 and 3) with $\gamma I_0 L=1$ (curve 2) and 2 (curve 3); $\Delta k_0\tau/\xi=-6$, $\xi L/\tau=20$. The inset illustrates narrowing of the main peak in the spectrum of the third harmonic with $\Delta\beta_0\tau/\xi=-1$ and $\xi L/\tau=2$ (curve 1), 4 (curve 2), and 10 (curve 3).

coupled into the fundamental HE_{11} mode of the PCF, phase matching, as shown by Fig. 1, is achieved for several adjacent high-order modes of the third harmonic. The THG phase-matching wavelengths for EH_{14}, TE_{04}, and EH_{52} modes of the considered fiber are 370, 425, and 438 nm, respectively. We can thus expect the appearance of multiplets of peaks in the spectrum of the third harmonic, representing phase-matched modes of the third-harmonic field.

We now apply a standard approach of the slowly varying envelope approximation (SVEA) [3] to analyze the spectrum of the third harmonic as a function of the pump-field parameters and the phase mismatch. The SVEA coupled equations for the envelopes of the pump and third-harmonic fields, $A(t,z)$ and $B(t,z)$, are written as

$$\left(\frac{\partial}{\partial t} + \frac{1}{v_p}\frac{\partial}{\partial z}\right)A = i\gamma_1 A|A|^2, \tag{5}$$

$$\left(\frac{\partial}{\partial t} + \frac{1}{v_h}\frac{\partial}{\partial z}\right)B = i\sigma(A)^3 \exp(-i\Delta\beta_0 z) + 2i\gamma_2 B|A|^2, \tag{6}$$

where v_p and v_h are the group velocities of the pump and third-harmonic pulses, respectively, and γ_1, γ_2, and σ are the nonlinear coefficients responsible for self-phase modulation (SPM), cross-phase modulation (XPM), and third-harmonic generation, respectively.

Solution of Eqs. (5) and (6) yields [5,6]

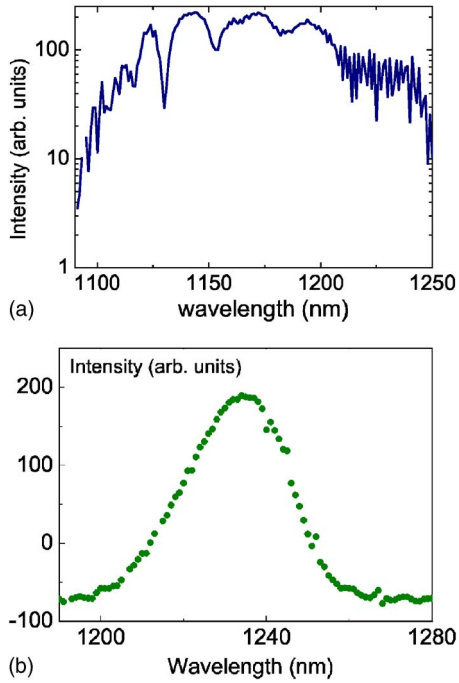

FIG. 3. (Color online) The spectrum of unamplified pump pulses with an input energy of 0.5 nJ transmitted through a PCF section with a length of 8 cm. The inset shows the input spectrum of pump pulses.

$$A(t_p,z) = A_0(t_p)\exp[i\varphi_{\mathrm{SPM}}(t_p,z)], \tag{7}$$

$$B(t_h,z) = i\sigma\int_0^z dz' A_0^3(t_h+\xi z')\exp[-i\Delta\beta_0 z' + 3i\varphi_{\mathrm{SPM}}(t_h+\xi z',z') + i\varphi_{\mathrm{XPM}}(t_h,z',z')], \tag{8}$$

where $t_l=(t-z/v_l)$ with $l=p,h$ for the pump and the field, respectively; $A_0(t)$ is the initial-condition envelope of the pump pulse; $\varphi_{\mathrm{SPM}}(t_p,z)=\gamma_1|A_0(t_p)|^2 z$ is the SPM-induced phase shift of the pump field; and $\varphi_{\mathrm{XPM}}(t_h,z',z)=2\gamma_2\int_{z'}^{z}|A_0(t_h+\xi z'')|^2 dz''$ is the XPM-induced phase shift of the third-harmonic field.

In the regime where the nonlinear phase shifts are small, the Fourier transform of Eq. (8) yields the following expression for the spectrum of the third-harmonic intensity:

$$I(\Omega,z) \propto \sigma^2 \frac{\sin^2[(\Delta\beta_0+\Omega\xi)z/2]}{(\Delta\beta_0+\Omega\xi)^2}\left|\int_{-\infty}^{\infty}\int_{-\infty}^{\infty} A(\Omega-\Omega') \times A(\Omega'-\Omega'')A(\Omega'')d\Omega' d\Omega''\right|^2, \tag{9}$$

where $A(\Omega)$ is the spectrum of the input pump field. In the regime of small nonlinear phase shifts, phase-matching effects can be thus decoupled from the influence of the spectrum of the pump field. While the phase matching is represented by the argument in the $\sin(x)/x$ function in the first factor on the right-hand side of Eq. (9), the significance of the pump spectrum is clear from the convolution integral appearing in this expression. Depending on the signs of the phase and group-velocity mismatch, $\Delta\beta_0$ and ξ, the peak in the spectrum of the third harmonic can be either red- or blueshifted with respect to the frequency $3\omega_0$. The spectral width of this peak, as can be seen from Eq. (9), is given by $\delta\approx 2\pi(|\xi|z)^{-1}$, decreasing as z^{-1} with the growth in the propagation coordinate z (the inset in Fig. 2).

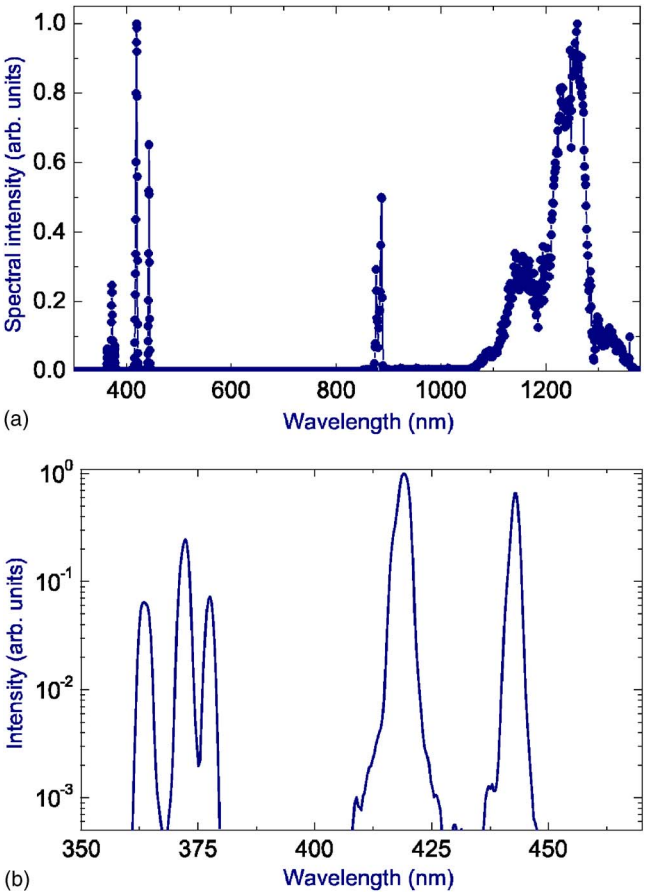

FIG. 4. (Color online) Output spectra for an 8-cm section of PCF with 0.5-nJ 60-fs Cr:forsterite laser pulses at the input of the fiber: (a) the total output and (b) the short-wavelength part of the spectrum.

With low pump powers, the generalized phase-matching condition of Eq. (3), as can be seen also from the exponential factor in Eq. (9), defines the central frequency $3\omega_0+\Omega_{\max}$, $\Omega_{\max}=-\Delta\beta_0/\xi$, of the peak in the spectrum of the third harmonic. The amplitude of this peak, as shown by Eq. (9), is determined by the amplitudes of the pump field components with frequencies $\omega_1=\omega_0+\Omega_{\max}-\Omega'$, $\omega_2=\omega_0+\Omega'-\Omega''$, and $\omega_3=\omega_0+\Omega''$, which can add up to transfer the energy to the $3\omega_0+\Omega_{\max}$ component in the spectrum of the third harmonic through the $\omega_1+\omega_2+\omega_3=3\omega_0+\Omega_{\max}$ process. The spectrum of the pump field should be thus broad enough to provide a high amplitude of this peak. In the regime when the SPM-induced broadening of the pump spectrum is small, the tunability range of the third harmonic (i.e., the range of frequency offsets Ω) is mainly limited by the bandwidth of the input pump field (curve 1 in Fig. 2). A similar spectral shift, limited to small Ω by a field-unperturbed pump spectrum and short interactions lengths, typical of nonlinear crystals, has

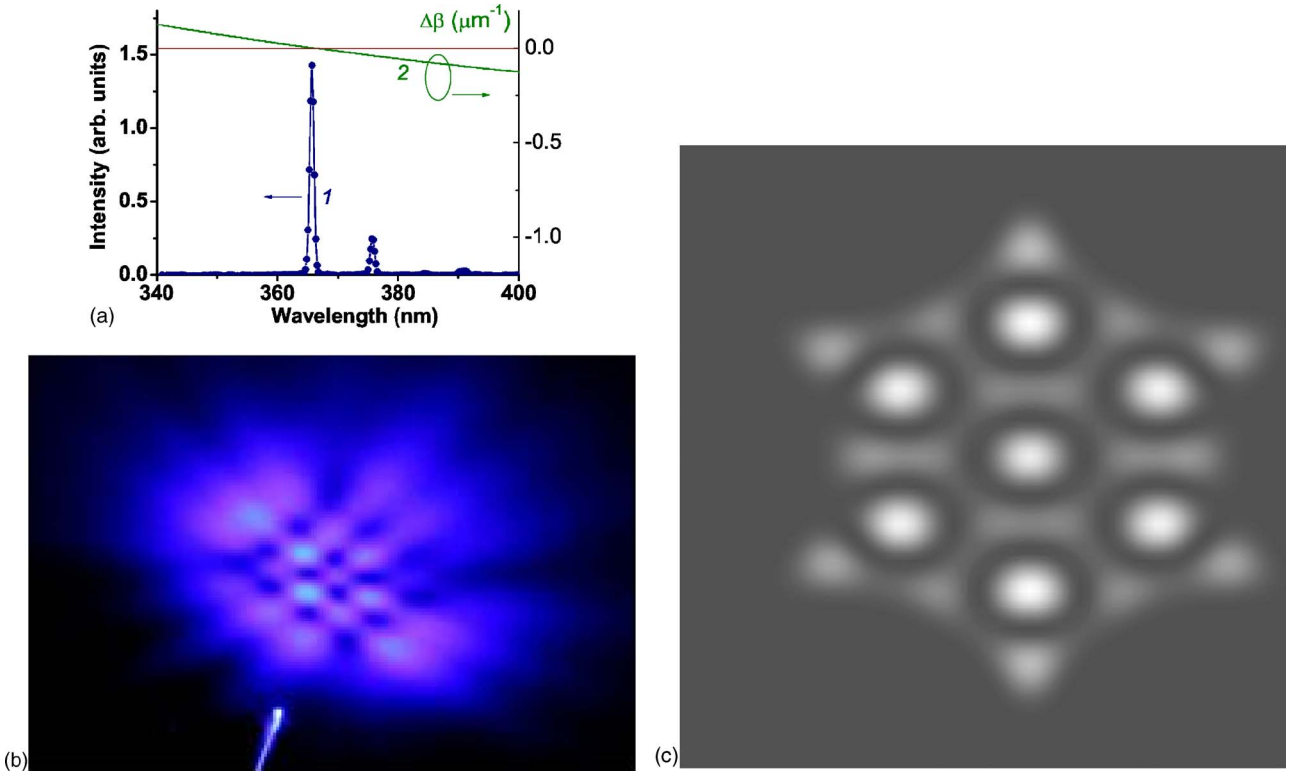

FIG. 5. (Color online) (a) Intensity spectrum of the blueshifted output of a 10-cm PCF with the energy of the input 60-fs Cr:forsterite laser pulse equal to 0.4 nJ (1) and the phase mismatch $\Delta\beta$ calculated for third-harmonic generation in the experimentally detected high-order PCF mode (2). (b) The field intensity profile in this signal. (c) The field intensity profile in the high-order PCF mode calculated with the use of the localized function expansion technique.

been earlier predicted by Akhmanov *et al.* [19] for second-harmonic generation.

Curves 2 and 3 in Fig. 2 illustrate the expansion of the tunability range of the third harmonic due to a SPM-induced spectral broadening of the pump field, examined by taking the Fourier transform of Eq. (8) including the nonlinear phase shifts. With $\gamma I_0 L=1$ [L is the interaction length, I_0 is the pump-field peak intensity, $\gamma I_0=\gamma_1|A_0(t_p=0)|^2$, $\gamma_2=3\gamma_1$], the spectrum of the pump field is broad enough to produce a high-amplitude peak at $\Omega_{\max}=-6/\tau$. The peak becomes narrower as the length of the nonlinear medium increases (cf. curves 1–3 in the inset to Fig. 2), suggesting a convenient way for an efficient generation of short-wavelength radiation with a well-controlled spectrum for spectroscopic and metrological applications. Generation of high-amplitude well-resolved narrowband third-harmonic peaks with large shifts Ω thus requires a mechanism for an efficient spectral broadening of the pump field. We will experimentally show below that this requirement can be satisfied with PCFs.

The laser setup employed in our experiments to study THG in PCFs was based on a femtosecond Cr:forsterite oscillator (described in detail elsewhere [20]), pumped by 1064-nm, 8.5-W radiation of a neodymium-doped yttrium aluminum garnet (Nd:YAG) laser system. The Cr:forsterite laser oscillator delivered 60-fs pulses of output radiation with a central wavelength of 1238 nm (see the inset in Fig. 3) and an average power in excess of 300 mW at a pulse repetition rate of 120 MHz. Both unamplified and amplified pulses of Cr:forsterite laser radiation were used as a pump for THG experiments in PCFs. For amplification, the laser pulses generated by the master oscillator were transmitted through a stretcher and an isolator, to be amplified in a Nd:YLF-laser-pumped amplifier and recompressed to the 110-fs pulse duration with the maximum laser pulse energy up to 40 μJ at 1 kHz.

The output laser beam was collimated with a 2× collimator and coupled into a PCF (shown in the inset to Fig. 1) placed on a three-dimensional translation stage using a 40 × microscope objective. A beam splitter and 10× objectives were employed to focus radiation coming out of the PCF onto the entrance slit of a Jobin-Yvon HR 640 spectrometer and the input of a fiber-coupled OceanOptics spectrometer, allowing both the infrared (up to 1.5 μm) and the uv-visible (from 255 nm) parts of the output spectrum to be simultaneously detected. With a coupling efficiency estimated as 30%, the typical energy of femtosecond pulses coupled into the fiber was about 0.5 nJ.

Figure 3 presents the spectrum of unamplified pump pulses with an input energy of 0.5 nJ transmitted through an 8-cm PCF sample with the cross-section structure shown in the inset to Fig. 1. As the pump pulse propagates through the PCF, it becomes spectrally broadened due to SPM and four-wave-mixing phenomena [21], providing a sufficient pump power density for THG within a broad spectral range. In Fig. 4(a), we present a typical total output spectrum recorded within a broad wavelength range for an 8-cm section of PCF with a 0.5-nJ pulse of the Cr:forsterite laser at the input of the fiber. This spectrum features a spectrally isolated group

of emission lines within the range of wavelengths from about 360 to 445 nm. A wide gap separating this group of spectral lines from the red part of the output radiation spectrum, with no emission observed within the range of wavelengths from 445 to 880 nm, emission in the 360–445 nm wavelength range cannot be interpreted as a part of the supercontinuum generation process. The spectral range where this blueshifted emission is observed suggests that this signal may originate from THG, which has been earlier identified [11–15,17] as one of the important processes contributing to nonlinear-optical spectral transformations of ultrashort pulses in PCFs.

As can be seen from a higher-resolution spectrum presented in Fig. 4(b), the short-wavelength part of the PCF output spectrum features three well-resolved groups of spectral peaks observed within the range of wavelengths from 361 to 445 nm, corresponding to approximately 150 THz in the frequency domain. The central wavelengths of these groups of peaks agree reasonably well with the results of our phase-matching analysis, presented in Fig. 1, indicating phase-matched THG in higher-order modes of the PCF. The complicated shape of the group of peaks observed in the (361–378)-nm wavelength region is attributed to phase matching achieved for orthogonally polarized guided modes, which have slightly different propagation constants because of the PCF birefringence.

To investigate the details of transverse field intensity distribution in the third-harmonic signal at the output of the PCF, we slightly change the experimental conditions by tilting the fiber axis with respect to the input laser beam in such a way as to generate a blueshifted output with a spectrum dominated by one high-intensity emission peak at 366 nm [curve 1 in Fig. 5(a)]. Figure 5(b) displays the field intensity profile in this signal, visualized by imaging the blue emission at the output of the PCF on a white screen. By comparing the measured field intensity profile with the results of our numerical simulations [Fig. 5(c)], performed with the use of the localized function expansion technique [22], we identify the beam pattern in Fig. 5(b) as the transverse field intensity distribution in one of the high-order PCF modes. Line 2 in Fig. 5(a) shows the results of localized-function calculations for the phase mismatch $\Delta\beta$ between the third harmonic generated in this mode and the fundamental mode of Cr:forsterite laser radiation used as a pump field. According to these calculations, the THG process in the considered PCF mode is phase matched at 367 nm, which agrees well with the experimental observation of an intense signal at 366 nm in the PCF output spectrum [line 1 in Fig. 5(a)].

The regime of THG illustrated by Figs. 5(a)–5(c) is very interesting both physically and methodologically, as it allows a reasonably accurate analysis of mode properties of the third-harmonic signal due to the simplicity of the third-harmonic spectrum, which is dominated by a single isolated spectral line [line 1 in Fig. 5(a)]. We have shown that this dominant peak in the blueshifted PCF output represents phase-matched THG in a high-order PCF mode. Typically, however, third-harmonic spectra include several high-amplitude peaks [Fig. 4(b)], corresponding to several PCF modes simultaneously phase matched for the given regime of nonlinear-optical interaction. Output beam patterns are quite complicated in that situation, as they represent a mixture of several high-order PCF modes, which makes the analysis of spatial mode properties of the output third-harmonic signal much less transparent and reliable. In particular, although we established a reasonable correlation between the modes that phase-match THG in the PCF (Fig. 1) and third-harmonic spectra at the output of the PCF [Fig. 4(b)], analysis of output beam profiles corresponding to Figs. 4(a) and 4(b) turns out to be not very productive in view of the complicated mixture of modes controlling the output beam pattern. We, therefore, restrict our discussion of this issue here to the methodologically transparent example of Figs. 5(a)–5(c).

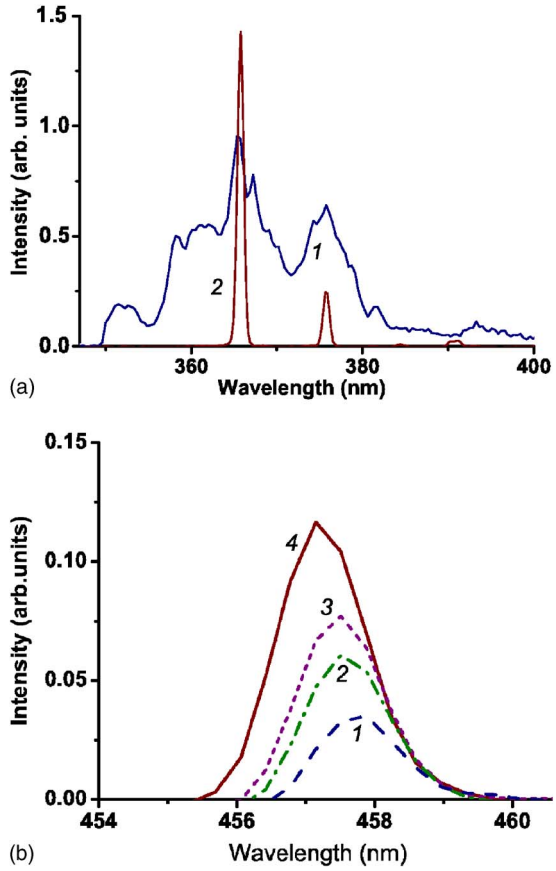

FIG. 6. (Color online) The spectra of a blueshifted component in the spectrum of the third harmonic generated by amplified 10-nJ Cr:forsterite laser pulses with an initial duration of 110 fs in a PCF with a length of (1) 6 and (2) 15 cm. The inset presents the spectra of one of the third-harmonic spectral components generated in a 1-μm-diameter waveguide channel in a 10-cm PCF by unamplified 60-fs pump pulses with different input energies: (1) 0.5, (2) 0.7, (3) 0.9, and (4) 1.1 nJ.

Expression (9) predicts a spectral narrowing of phase-matched frequency-shifted peaks in the spectrum of the third harmonic with the growth in the interaction length. To observe this effect, we compared the spectra of the third harmonic generated in 6- and 15-cm PCFs by amplified Cr:forsterite laser pulses with an initial duration of 110 fs and an input energy of 10 nJ. The results of this comparison are presented in Fig. 6. The spectral peaks centered at 365 and 376 nm tend to become narrower in longer PCFs, forming a doublet of well-resolved narrowband signals for PCFs longer than 15 cm. This behavior of the spectral features of the third

harmonic generated in the PCF agrees very well with our theoretical analysis.

In the presence of a strong pump field, the phase-matching condition of Eq. (3) should be modified to include the SPM- and XPM-induced nonlinear phase shifts. With $\gamma I_0=\gamma_1|A_0(t_p=0)|^2$ and $\gamma_2=3\gamma_1$, this field-corrected phase-matching condition yields $\Omega(P)=-(\Delta\beta_0+3\gamma P)/\xi$, where P is the pump peak power. For a typical situation of small-core fused silica waveguide channels and PCFs with $\Delta\beta_0>0$, $\xi<0$, and $\gamma>0$, the Kerr noninearity leads to a blueshifting of phase-matched peaks in the spectrum of the third harmonic with the growth in the pump intensity. This effect is observed for the third harmonic generated by unamplified 60-fs Cr:forsterite laser pulses in small-diameter fused silica waveguide channels in the PCF cladding off the central fiber core. A strong confinement of the laser field in these high-index-step small-diameter waveguides substantially enhances the nonlinearity [23–25], giving rise to large nonlinear phase shifts of the pump and third-harmonic fields. The increase in the energy of the pump pulses under these conditions leads to a substantial blueshifting of third-harmonic peaks, in accordance with the field-corrected phase-matching condition (see the inset in Fig. 6). The maximum efficiency of THG, defined as the ratio of the total energy of radiation emitted within the (361–460)-nm wavelength range to the energy of the input pump pulse, was estimated as 0.5% in these experiments.

The experimental results presented in this paper demonstrate that PCFs are ideally suited for non-3ω THG, allowing efficient tunable frequency up-conversion based on this phenomenon. PCFs possess a unique combination of properties required to achieve large frequency shifts Ω, still providing large amplitudes of spectrally shifted peaks with almost no energy converted to the frequency $3\omega_0$. Dispersion of guided modes in PCFs can be tailored by changing the structure of the fiber [10], helping, as shown above, to achieve phase matching for a given frequency of the pump field. PCFs can provide the maximum waveguide enhancement of nonlinear-optical processes [23–25] due to the strong confinement of the field in a small-size fiber core and a high-refractive-index step between the core and the cladding. This enhanced nonlinearity leads to an efficient spectral broadening of the pump field (which typically involves not only SPM, but also a variety of PCF-enhanced nonlinear processes; see, e.g., [26] for a review), expanding the spectral range around the frequency $3\omega_0$ where high-amplitude Ω-shifted peaks can be generated. Finally, large interaction lengths typical of PCFs not only result in high THG conversion efficiencies, but also, as shown in the previous section, help to produce spectrally isolated narrowband Ω-shifted peaks around the frequency $3\omega_0$, serving as a source of high-spectral-quality blue visible and ultraviolet radiation.

We are grateful to Yu. N. Kondrat'ev, V. S. Shevandin, K. V. Dukel'skii, and A. V. Khokhlov for fabricating fiber samples. This study was supported in part by the Russian Federation for Basic Research (Projects No. 03-02-16929, No. 04-02-81036-Bel2004, No. 04-02-39002-GFEN2004, and No. 03-02-20002-BNTS-a), the Russian Federal Research and Technology Program (Contract No. 02.434.11.2010), and INTAS (Projects No. 03-51-5037 and No. 03-51-5288). The research described in this publication was made possible in part by Award No. RP2-2558 of the U.S. Civilian Research & Development Foundation for the Independent States of the Former Soviet Union (CRDF). Collaborative research of International Laser Centers in Moscow and Bratislava is a part of COST P11 action of European Science Foundation.

[1] S. Chandrasekhar, *Hydrodynamic and Hydromagnetic Instability* (Clarendon, Oxford, 1961).
[2] L. D. Landau and E. M. Lifshitz, *Fluid Mechanics* (Pergamon, New York, 1966).
[3] Y. R. Shen, *The Principles of Nonlinear Optics* (Wiley, New York, 1984).
[4] N. Bloembergen, *Nonlinear Optics* (Benjamin, New York, 1965).
[5] N. I. Koroteev and A. M. Zheltikov, Appl. Phys. B: Lasers Opt. **67**, 53 (1998).
[6] A. N. Naumov and A. M. Zheltikov, Opt. Express **10**, 122 (2002).
[7] J. C. Knight, T. A. Birks, P. St. J. Russell, and D. M. Atkin, Opt. Lett. **21**, 1547 (1996).
[8] J. C. Knight, J. Broeng, T. A. Birks, and P. St. J. Russell, Science **282**, 1476 (1998).
[9] P. St. J. Russell, Science **299**, 358 (2003).
[10] W. H. Reeves, D. V. Skryabin, F. Biancalana, J. C. Knight, P. St. J. Russell, F. G. Omenetto, A. Efimov, and A. J. Taylor, Nature (London) **424**, 511 (2003).
[11] J. K. Ranka, R. S. Windeler, and A. J. Stentz, Opt. Lett. **25**, 796 (2000).
[12] F. G. Omenetto, A. Taylor, M. D. Moores, J. C. Knight, P. St. J. Russell, and J. Arriaga, Opt. Lett. **26**, 1558 (2001).
[13] A. Efimov, A. J. Taylor, F. G. Omenetto, J. C. Knight, W. J. Wadsworth, and P. St. J. Russell, Opt. Express **11**, 910 (2003).
[14] A. Efimov, A. J. Taylor, F. G. Omenetto, J. C. Knight, W. J. Wadsworth, and P. St. J. Russell, Opt. Express **11**, 2567 (2003).
[15] F. G. Omenetto, A. Efimov, A. J. Taylor, J. C. Knight, W. J. Wadsworth, and P. St. J. Russell, Opt. Express **11**, 61 (2003).
[16] S. O. Konorov, A. A. Ivanov, M. V. Alfimov, A. B. Fedotov, Yu. N. Kondrat'ev, V. S. Shevandin, K. V. Dukel'skii, A. V. Khokhlov, A. A. Podshivalov, A. N. Petrov, D. A. Sidorov-Biryukov, and A. M. Zheltikov, Laser Phys. **13**, 1170 (2003).
[17] A. N. Naumov, A. B. Fedotov, A. M. Zheltikov, V. V. Yakovlev, L. A. Mel'nikov, V. I. Beloglazov, N. B. Skibina, and A. V. Shcherbakov, J. Opt. Soc. Am. B **19**, 2183 (2002).
[18] D. A. Akimov, A. A. Ivanov, A. N. Naumov, O. A. Kolevatova, M. V. Alfimov, T. A. Birks, W. J. Wadsworth, P. St. J. Russell, A. A. Podshivalov, and A. M. Zheltikov, Appl. Phys. B: Lasers Opt. **76**, 515 (2003).

[19] S. A. Akhmanov, A. P. Sukhrukov, and A. S. Chirkin, Zh. Eksp. Teor. Fiz. **55**, 1430 (1968).
[20] A. A. Ivanov, M. V. Alfimov, and A. M. Zheltikov, Phys. Usp. **174**, 743 (2004).
[21] G. P. Agrawal, *Nonlinear Fiber Optics* (Academic, Boston, 1989).
[22] T. M. Monro, D. J. Richardson, N. G. R. Broderick, and P. J. Bennet, J. Lightwave Technol. **18**, 50 (2000).
[23] A. M. Zheltikov, Opt. Spectrosc. **95**, 410 (2003).
[24] D. A. Akimov, E. E. Serebryannikov, A. M. Zheltikov, M. Schmitt, R. Maksimenka, W. Kiefer, K. V. Dukel'skii, V. S. Shevandin and Yu. N. Kondrat'ev, Opt. Lett. **28**, 1948 (2003).
[25] M. A. Foster, K. D. Moll, and A. L. Gaeta, Opt. Express **12**, 2880 (2004).
[26] W. J. Wadsworth, A. Ortigosa-Blanch, J. C. Knight, T. A. Birks, T. P. M. Mann, and P. St. J. Russell, J. Opt. Soc. Am. B **19**, 2148 (2002).